Malaysian Journal of Chemistry, 2025, Vol. 27(3), 499-508
(Special Issue: *International Conference on Sustainable Materials and Technologies, ICSMT 2025*)

Optimizing Fiber-Matrix Interaction: Impact of Plasma Treatment on Abaca and Kenaf Polymer Composites

Velliyangiri, B.*, Rajavignesh, S., Pugazhendhi, K. and Manoranjan, T.
Department of Mechanical Engineering, Nandha Engineering College, Perundurai 638052,
Tamil Nadu, India
*Corresponding author (e-mail: bvelliyangiri@gmail.com)

Epoxy composites reinforced with abaca (AF) and kenaf (KF) fibers were the focus of this investigation. Both fibers were exposed to plasma from a dielectric barrier discharge (DBD) for processing time of 5 to 25 minutes. Epoxy resin mixes with AF or KF were not necessary for plasma treatment. The plasma-treated fibers' infrared spectra revealed amplified carboxyl group peak intensity in the Fourier transform. The tensile strength of Epoxy/AF treated for 20 minutes reached 60.8 MPa, whereas the elongation at break of Epoxy/KF treated for the same amount of time increased by 6.4%. Flexural testing showed that kenaf composites, when treated with plasma, had a much higher flexural strength (up to 62.2 MPa) than abaca composites. Both composites benefited from plasma treatment, which improved surface coarseness and fiber interactive adhesion. The DBD plasma treatment enhanced the material's thermal stability and wettability. The composites' mechanical, thermal, and water contact angle (WCA) characteristics were enhanced by the dielectric barrier discharge treatment, which improved the interaction bonding of the fibers and matrix.

Keywords: Abaca; Kenaf; Epoxy composites; Plasma treatment; Flexural tests

Received: February 2025; Accepted: May 2025

As a result of their adaptability, bio-composites have gained popularity in a number of markets in recent years. Because they combine the strengths of polymers with reinforcing elements, they are environmentally benign material alternatives to petroleum-based polymers [1]. Polymers that have been reinforced with biomaterials show improved chemical, thermal, and mechanical characteristics. A reinforcing phase is mixed with a polymer matrix to create a composite. Lightweight, sturdy, and long-lasting buildings are the end product of this method [2]. Various technical applications have begun to incorporate cellulose fibers as reinforcement materials in polymer composites owing to their recyclability, low cost, density, and maximum mechanical characteristics [3]. Fibers made of cellulose are renewable, safe, and easy on the planet. Abaca fibers have been promoted as a viable alternative to reinforcing materials in various manufacturing sectors, including packaging, construction, automotive, and furniture [4].

The hollow cylindrical structure of abaca is the result of its composition of a sequence of internodes and nodes. Abaca fibers have a high tensile strength, high stiffness, and a cellulose content of up to 40 to 50% and the lignin level is 20 to 30 % [5]. Because of its unique chemical composition, abaca is both a strong and flexible material with many potentials uses in building and industry. Fiber reinforcement in polymer composites makes use of abaca fibers (AF), which are byproducts of the processing of abaca [6]. The tensile strength of these fibers is great, on par with that of certain synthetic fibers. The light weight structure, strength, and biodegradability of abaca fiber composites make them a popular choice for construction, automotive components, and packaging [7]. Composite reinforcement can also be made from kenaf, another natural material. Since they are strong, lightweight, and have outstanding thermal properties, kenaf fibers (KFs) are an excellent choice for composites that require heat stability and durability [8]. Owing to its composition of cellulose (65 to 75 %), lignin (6 to 9 %) and hemicellulose (10 to 20 %), KF possesses excellent mechanical characteristics. For a very long time, kenaf has been an essential component of numerous textiles. Those involved in eco-friendly production know it well for its reinforcing fiber applications in polymer composites [9].

Composites have many potential uses, but complications with compatibility and the hydrophobic nature of resins and natural fibers restrict their widespread use. Natural fibers and matrix resins are treated with surface treatments using physical and chemical approaches to improve the interfacial adhesion [10]. A lot of research has gone into finding ways to modify surfaces chemically, physically, or otherwise to make them stick better to one another. Acid, silane, plasma, and enzymatic treatments are some of the most

---

†Paper presented at the International Conference on Sustainable Materials and Technologies(ICSMT 2025)

common ways to modify surfaces [11]. In order to increase the transfer load among the matrix and the fiber, these treatments either roughen the fiber's surface or add functional groups that strengthen the adhesion. Building, automotive, and packaging sectors are seeing a rise in the use of natural fiber composites owing to its biodegradability, strength, and lightweight construction [12]. Materials undergo plasma treatment by exposing them to a gas that is partially ionized, along with electrons, ions, and neutral particles.

Plasma and surface interaction alters materials in a variety of ways, including chemical, physical, and structural changes. Atmospheric plasma therapy using dielectric barrier discharge (DBD) plasma involves separating two electrodes by a dielectric barrier [13]. At atmospheric pressure, this configuration ensures that non thermal plasma is generated uniformly. Natural fibers are commonly treated with DBD plasma because of its scalability and energy efficiency. The gasses employed in the DBD plasma might range from oxygen to nitrogen to argon, depending on the type of surface alteration that is needed. A novel approach to surface enhancement of natural fibers with DBD plasma enables the creation of chemical and physical cross links with the polymer matrix through the enhancement of reactive functional groups and surface roughness, respectively [14]. Enhanced polymer composites through synergistic cross linking have a wide range of potential uses [15]. Epoxy resin's (ER) chemical resilience, exceptional mechanical properties, and electrical insulation make it an invaluable tool for engineers. The reaction of curing agents like amines, anhydrides, or phenols and epitaxes produces ERs. The distinctive strength and durability of epoxy are produced when the material cures, when a hard cross linked network structure is formed [16].

An epoxy matrix is reinforced with high-strength fibers to create a fiber-reinforced epoxy composite [17]. The mechanical qualities of the composite material are better than those of the constituent parts because of this combination. Epoxy creates a matrix that secures the fibers, evens out their stress, and shields them from harm. Reinforcing materials like fibers give strength and stiffness [18]. Some scientists tried to create natural fiber-reinforced epoxy without changing the surface, but the resulting material had poor mechanical qualities and a connecting phase that separated the fibers from the epoxy. Prior to blending with an epoxy matrix, one aims to enhance the surface of the fibers using chemical and physical techniques [19]. Enhancing the chemical and physical roughness of the fiber surface enhances the blend's response, interfacial adhesion, and characteristics.

This study used plasma technology to modify the surface of AF and KF using a combination of physical and chemical procedures, improving their surface quality. Plasting the fibers in an NH_4OH solution after plasma-treating them with an argon + oxygen gas ($Ar + O_2$) for various periods ranging from 0 to 25 minutes improved their chemical structure. Using NH_4OH, $-NH_2$ groups were grafted onto the fibers, altering their surface structure. Epoxy groups are capable of reacting with these groups. The DBD plasma process enhanced the fibers' polarity and surface roughness. The characteristics of the two fiber composites were elucidated. We used flexural and tensile strength measurements, together with Fourier-transform infrared spectroscopy (FTIR) to look at chemical attachment and reactions, to find out how the plasma treatment affected the composites. For the purpose of determining the structural and functional effects of plasma treatment, scientists monitored the composite's heat stability and shape. This study sheds light on the possibility of using plasma treatment on natural fiber composites to make environmentally friendly materials that are both stronger and more long-lasting for use in industrial settings.

EXPERIMENTAL MATERIALS AND METHODOLOGY

Materials

The abaca fibers were supplied by fiber source enterprises in Chennai, Tamilnadu, India. The KFs were obtained from Go Green Enterprises in Chennai, Tamil Nadu (TN), India. Kovaicheenu enterprises, Coimbatore, Tamilnadu, India provided the epoxy and hardener. The ammonium hydroxide (NH_4OH), sodium chlorite ($NaClO_2$), and sodium hydroxide (NaOH), required for the surface modification were purchased from the local chemical shop in Erode, TN, India.

Fiber Treatment

The abaca and kenaf fibers were subjected to a mild alkaline treatment in a 20 % w/v aqueous NaOH solution for six hours prior to plasma treatment. In order to eliminate lignin and hemicellulose, the pulps were bleached using $NaClO_2$ [20]. A 180 µm sieve was used to filter the fibers. Surface alteration of the abaca and kenaf fibers was achieved by the use of a DBD plasma method. The DBD was made by placing the fibers on a tray and connecting two equivalent maximal power rods, which were insulated by a thin layer of foil. The fiber discharge gap can be fine-tuned by adjusting the grounded electrode. A continuous frequency of 13.56 kHz and a high-voltage power of 200 W were used to generate the DBD plasma. Argon and oxygen gas were used to reach 10 and 12 L/min plasma flow rates, correspondingly. The kenaf and abaca fibers were subjected to the DBD plasm for 4, 8, 12, 16, and 20 minutes, respectively. The surface of the treated fibers was altered by combining them with an

NH_4OH solution (1:10% w/v) at each plasma setting. For 90 minutes, the sample was heated on a hot plate to 80ºC while being swirled constantly. The resulting product was then heated to 80ºC for two days to evaporate the NH_4OH solution.

Table 1. Composition of composites samples.

Specimen	**Epoxy Resin (wt%)**	**Type of Fiber**	
		AF (wt %)	**KF (wt %)**
Epoxy / $AF_{untreated}$	90	10	0
Epoxy / $AF_{treated}$4%	90	10	0
Epoxy / $AF_{treated}$8%	90	10	0
Epoxy / $AF_{treated}$12%	90	10	0
Epoxy / $AF_{treated}$16%	90	10	0
Epoxy / $AF_{treated}$20%	90	10	0
Epoxy / $Kenaf_{untreated}$	90	0	10
Epoxy / $Kenaf_{treated}$4%	90	0	10
Epoxy / $Kenaf_{treated}$8%	90	0	10
Epoxy / $Kenaf_{treated}$12%	90	0	10
Epoxy / $Kenaf_{treated}$16%	90	0	10
Epoxy / $Kenaf_{treated}$20%	90	0	10

Fabrication of Composites

According to Table 1, fiber composites were created utilizing a hand layup process with a 10:1 combination of epoxy and hardener. Before combining the abaca and kenaf fiber samples with epoxy at room temperature, the fiber composites were divided into two groups: one that had been treated with plasma and another that had untreated. While an inhaled vacuum was used to eliminate air bubbles from the epoxy, the mixed samples were agitated to improve the fiber dispersion. After being poured into a bone-shaped silicone mold, the liquid was dried at 85°C for 5 hours.

FTIR Spectroscopy

An analysis was conducted on the materials' chemical functional groups utilizing ATR mode Fourier transform infrared spectroscopy (FTIR). The range of 400 to 4000 $cm^{-1}$was covered by the FTIR spectra, which were acquired using 32 scans with a 4 cm^{-1} scan resolution.

Tensile Properties

Samples with a dog bone shape have size of 250×25×3 mm. The test followed the JISK-6251-7 protocol (Model MCT1150, Tokyo, Japan) and was performed at room temperature. Both the tensile strength (TS) and the elongation at break (EB) were tested at a crosshead speediness of 50 mm min^{-1}.

Flexural Test

A silicone mold that conformed to the ASTM standard, with size of 125 mm × 12 mm × 3 mm, was employed to hold the samples. It contained a 3-point bending test with a 1 kN force at ambient temperature. For the analysis, the mean of five samples was considered. The following methods were employed to ascertain the modulus and flexural strength [21]:

$$\text{Flexural strength} = \frac{3FL}{2bd^2}, \quad (1)$$

$$\text{Flexural modulus} = \frac{mL^3}{4bd^3} \quad (2)$$

Whereas F is the maximum failure load in N, L denotes span length in mm, b denotes width, d represents thickness, and m indicates slope of the load vs. displacement curvature to the beginning line.

Microstructural Analysis

To analyze the fracture morphology of the specimen, ZEISS scanning electron microscopy (SEM) was used. A hot air oven was used to evaporate the liquid nitrogen from the impact fracture surface after shattering it for 90 minutes at 80ºC. Under a vacuum, the samples were examined after being sputtered with gold at a voltage of 15 kV.

Thermal Properties

The thermo gravimetric testing of the thermal stability of the epoxy and fiber strengthened epoxy was conducted in a nitrogen atmosphere. The testing temperature ranged from 50 to 550°C, at 10°C/min [22].

Contact Angle

Utilizing a water droplet instrument (DSA30E, Kruss Co., Ltd., Hamburg, Germany), the water contact angle (WCA) was obtained. The samples were made by casting the silicone molds and then connecting them to glass slides [23]. Over the course of 0 to 10 minutes, the shape of the water droplet was recorded. Each sample had its water contact angles tested five times before an average was determined.

RESULTS AND DISCUSSIONS

FTIR Analysis

Figure 1(a) and Figure 1(b) displays the outcomes of a Fourier transform infrared spectroscopy investigation into the chemical composition of DBD plasma-treated fiber-reinforced epoxy composites using abaca and kenaf fiber. Fibers that were treated and those that were not displayed stretching vibrations of hydroxyl (O−H) between 3262 and 3358 cm−1. Bands at 2899 $cm^{-1}$and 1642 cm^{-1}were used to identify alkane functional groups on cellulose fiber and aromatic groups on lignin, respectively. A signal at 1741 cm^{-1}showed that the acetyl groups in hemicellulose were carbonyl (C=O) stretched. The highest lignin loss was seen at 1653 cm^{-1}in both the treated and untreated fibers. This was due to the NaOH treatment and blanching that occurred prior the plasma treatment [24]. In the Epoxy/AF and Epoxy/KF composites, we detected Carbon−Carbon stretch peak at 1627 and 1603 cm^{-1}, together with Carbon=Carbon stretch vibrations of the epoxy at 1523 and 1470 cm^{-1}. The observed stretching modes of the oxirane ring are as follows: C−O symmetrical stretching

at 1241 cm^{-1}, C−O asymmetrical stretch at 920 cm^{-1}, and C−O∗C stretching at 833 cm−1. The O−H stretching of the fibers' hydroxyl groups caused the composites treated with plasma to show an enhanced maximum intensity at 3300 to 3700 cm^{-1}. During the Ar + O_2 gas treatment, polar groups at 1680 to 1720 cm^{-1} were produced by carbonyl (C=O) and carboxyl (−COOH). It was also observed that the carbon hydrogen group (CH2, CH3) was stretched between 2850 and 3000 cm^{-1}. The number of surface oxygen comprising groups grew due to the fiber-resin link as the plasma treatment advanced. The Epoxy/$AF_{treated}$ composite, in contrast, did not show any epoxy groups at 918 cm^{-1}.

After 20 minutes of treatment, the innovative high peak at 1800 cm^{-1}that developed in the Epoxy/$AF_{treated}$ composites vanished. The formation of a new C−O bond, possibly as a consequence of the epoxy reacting with the AF surface, is shown by the appearance of a new peak after 20 minutes of treatment. The C=O stretching vibrations at 1469 $cm^{-1}$and COOH at 1842 cm^{-1}were observed in untreated KF. The increasing amount of hydroxyls and Carbon−Oxygen groups on the surface of KF caused both peaks to intensify as the treatment continued. The evidence in the data points to a relationship between the −COOH groups, NH_4OH, and epoxy groups composed of epoxy. When the epoxy was added, the −COOH groups vanished. Through interactions with epoxy groups, the data also show that $-NH_2$ groups graft onto the surfaces of the fibers. As the time of plasma treatment improved, the Epoxy/KF composites' epoxy group intensity at 1021 cm^{-1} decreased due to the rapid response of the KF surface and matrix [25]. The reactive functional groups on the fibers' surfaces are enhanced through plasma treatment; these groups react with the epoxy clusters in the primary matrix of the epoxy. The abaca and kenaf fibers' chemical and physical structural characteristics were changed by plasma treatment. Thus, matrix-fiber interaction and interfacial adhesion were caused by the generation of efficient groups. It is possible that these interactions are the reason why composites have better properties.

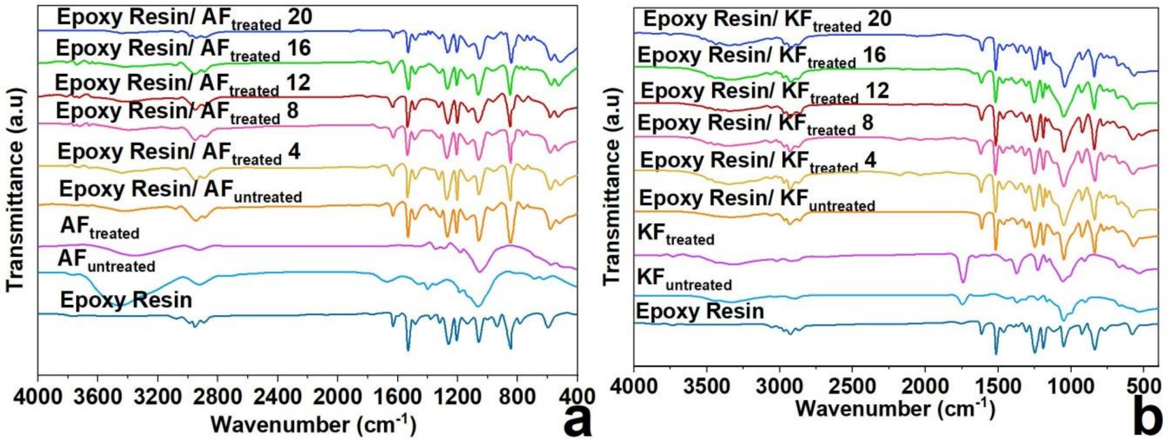

Figure 1. FTIR analysis of (a) abaca and (b) kenaf fiber-reinforced epoxy composites.

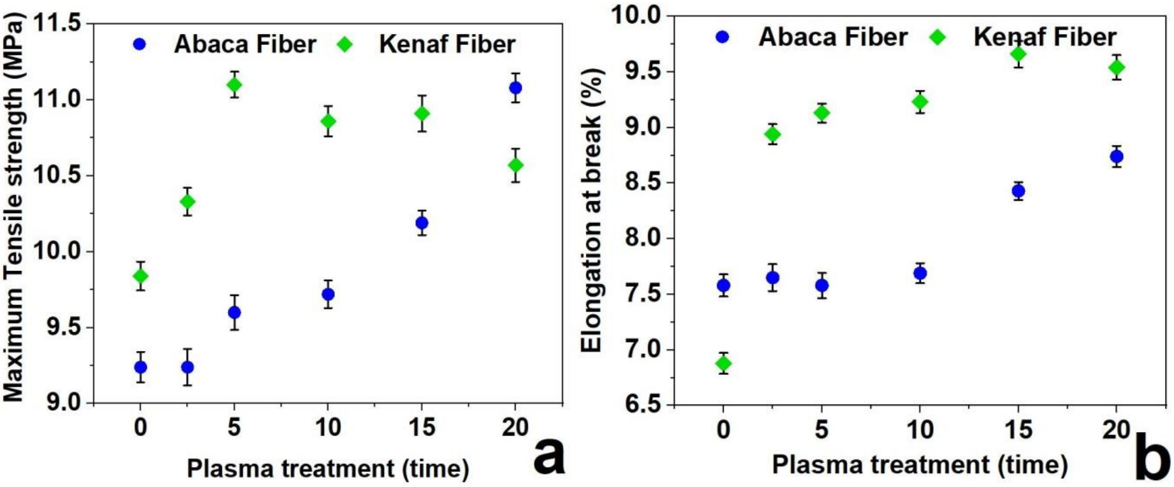

Figure 2. Evaluation of tensile properties of abaca and kenaf fiber-reinforced epoxy composites (a) Maximum tensile strength and (b) elongational break.

Tensile Properties

Figure 2(a) and Figure 2(b) displays the tensile characteristics of AF and KF epoxy treated with plasma for 0-20 minutes. The EB was 4.7% and the TS was 42 MPa for the Epoxy/AF$_{untreated}$ composite, which contained untreated abaca fibers. The EP/AF$_{treated}$ composites showed an increasing trend in TS and EB after being treated with NH_4OH gas for 4-20 minutes. Their maximum tensile strength was 60.8 MPa, which they exhibited twenty minutes later. The TS of the Epoxy/KF$_{untreated}$ composite was 48.3 MPa, and the elongation at break was 3.6%, as compared to untreated kenaf. Tensile strengths were higher in the EP/KF$_{treated}$ composites compared to the untreated composite (peaking at 60.8 MPa after 5 minutes), albeit they did decline marginally as treatment duration increased. The EP/KF$_{treated}$ composite's elongation at break increased from 3.6% to 6.4% as the treatment duration increased. Epoxy composites strengthened with abaca and kenaf fibers exhibited higher tensile strengths, which we attributed to the fibers' interaction with the epoxy matrix. The effectiveness of the adhesive bond between the epoxy and reinforced fibers was greatly affected by the plasma treatment of the fibers. Reinforcement with kenaf enhanced elongation at break in the samples, but reinforcement with abaca increased tensile strength more noticeably [26]. Plasma etching raised the surface roughness, which stimulated diffusion and penetration at the fiber-matrix interface and resulted in the creation of interlocking connections. Composites may have enhanced mechanical capabilities as a result of physical cross linking involving highly roughened fibers and a high level of interfacial chemical interaction between epoxy and -COOH groups of fibers. The mechanical characteristics of the composites show the ideal plasma processing settings.

Table 2. The results on flexural properties of the raw and plasma treated composites.

Specimen	Abaca fibers (AF)		Kenaf fibers (KF)	
	FS (MPa)	FM (GPa)	FS (Mpa)	FM (GPa)
Epoxy / Untreated	57.83	12.03	58.63	12.13
Epoxy / Treated 4%	56.53	11.43	57.83	12.03
Epoxy / Treated 8%	53.03	11.13	50.83	10.83
Epoxy / Treated 12%	58.73	13.03	59.93	12.83
Epoxy / Treated 16%	60.43	12.93	57.03	12.83
Epoxy / Treated 20%	61.63	12.13	67.73	13.03

Flexural Test

Our assessment of the flexural strengths of the composites, using abaca and kenaf fibers treated with plasma is presented in Table 2. Both the FM and FS of the abaca untreated composite, Epoxy/$AF_{untreated}$, are 10.2 GPa and 58.4 MPa, respectively. Flexural moduli were 6.9 GPa, flexural strengths (FS) were 60.5 MPa, flexural moduli (FM) were 56.2 GPa, and flexural strengths were 62.2 MPa for Epoxy/$AF_{treated}$ samples treated for 2.5, 5, 10, 15, and 20 minutes, respectively. As for the flexural strength modulus, it was 60.5 MPa for the Epoxy/$KF_{untreated}$ composite and 7.6 GPa for the untreated one. The moduli (10.2,9.3, 7.8, 10.3, and 11.1 GPa) and flexural strengths (59.3, 53.6, 62.2, 54.4, and 68.3 MPa) of the kenaf fiber-reinforced composites demonstrated rising trends with treatment time after plasma treatment, which is attributed to the improvements in $KF_{treated}$ roughness and interfacial adhesion of the Epoxy/$KF_{treated}$ composites. After being treated with DBD plasma and O_2 gas, the mechanical properties of abaca and kenaf were improved. The kenaf fibers outperformed the abaca fibers in terms of FS and FM because of their unique chemical composition and structural responsiveness to plasma treatment [27].

Microstructural Analysis

Scanning electron microscopy was used to capture images of the fractured composite surfaces. Figure 3(a) to Figure 3(l) displays the outcomes of plasma treatment in comparison to untreated variants of various abaca and kenaf-structured fiber-reinforced epoxy composites. The treatments varied in length. Abaca fibers with a smooth surface were present in both the Epoxy/AFtreated4 sample and the Epoxy/$AF_{untreated}$ composite. The oxygen in the discharge gases induced oxygen groups, which resulted in a noticeably coarser fiber structure, when the plasma treatment period was extended from 4 to 20 minutes. The surface becomes uneven due to chemical species formation and etching caused by plasma treatment. The inclusion of fine AF- and KF-treated fibers dispersed throughout the epoxy matrix improved the composite's characteristics.

Because the abaca fiber-reinforced composites were plasma treated with O_2 gas, which etched the surface and reduced the fiber's polarity through the production of oxygen bonding, the gaps between the fibers and matrix were quite apparent. The enhanced tensile strength was associated with a decrease in gaps between the AF surface and epoxy matrix after 20 minutes of plasma treatment. Having said that, the tensile strength was reduced in the Epoxy/$KF_{treated}$ 20 samples, likely as a result of the deterioration of the KF fiber, which had a weaker structure than the AF fiber. The gaps between the KF and epoxy matrix were also minimal. A small reduction in tensile strength was achieved through a combination of fiber degradation and interfacial cross linking [28]. Compared to the abaca fibers, the KF-reinforced composites displayed distinct features in the scanning electron micrographs. Untreated Epoxy/$KF_{untreated}$ composite fiber morphology showed kenaf stem sections with smooth fibers, big pores, and an uneven structure. Because KF and BR had a strong interfacial adhesion thanks to the physical and chemical changes made to the KF surface, the EP/$KF_{treated}$ composites showed minimal gaps between the KF and BR matrix during the whole treatment period. Composites treated with epoxy and KF demonstrated surface improvements without fiber removal, owing to the strong bond between the two materials. Changes in fiber surface etching, a rise in surface roughness, and the induction of –COOH groups on the KF structure were all outcomes of the ion bombardment, etching, and layer ablation performed by the DBD plasma. As a result of the cross linking reaction, the composites' mechanical properties and interfacial adhesion were improved after prolonged treatment.

Thermal Properties

Various amounts of time were used to conduct thermal analyses on pure epoxy, fiber-strengthened epoxy composites with raw fibers, and fibers that had been plasma-treated. The results of these analyses are displayed in Figure 4(a) and Figure 4(b). In the first step, at around 150ºC, the epoxy begins to lose weight as a result of the released humidity from the composites.

Throughout the course of treatment, the Epoxy/AF and Epoxy/KF composites exhibited similar characteristics. Compared to pure ER, the epoxy blend containing fibers lost more weight in the 200 to 350ºC temperature range, and this disparity became even more noticeable with increasing treatment period. The fibers of all the composites degraded at 370ºC because the cellulose and hemicellulose in them broke down. Decomposition of the lignin phase occurred between 400 and 460ºC, resulting in a 6% reduction in weight. The breakdown of hemicellulose, cellulose, and lignin requires a greater temperature. An ash content that increased with treatment duration was seen in the residual component at 500 to 600ºC, which was caused by the maximal degree of cross-linking response surrounding the fiber-epoxy interface. Composites' mechanical properties and interfacial adhesion were improved through cross linking.

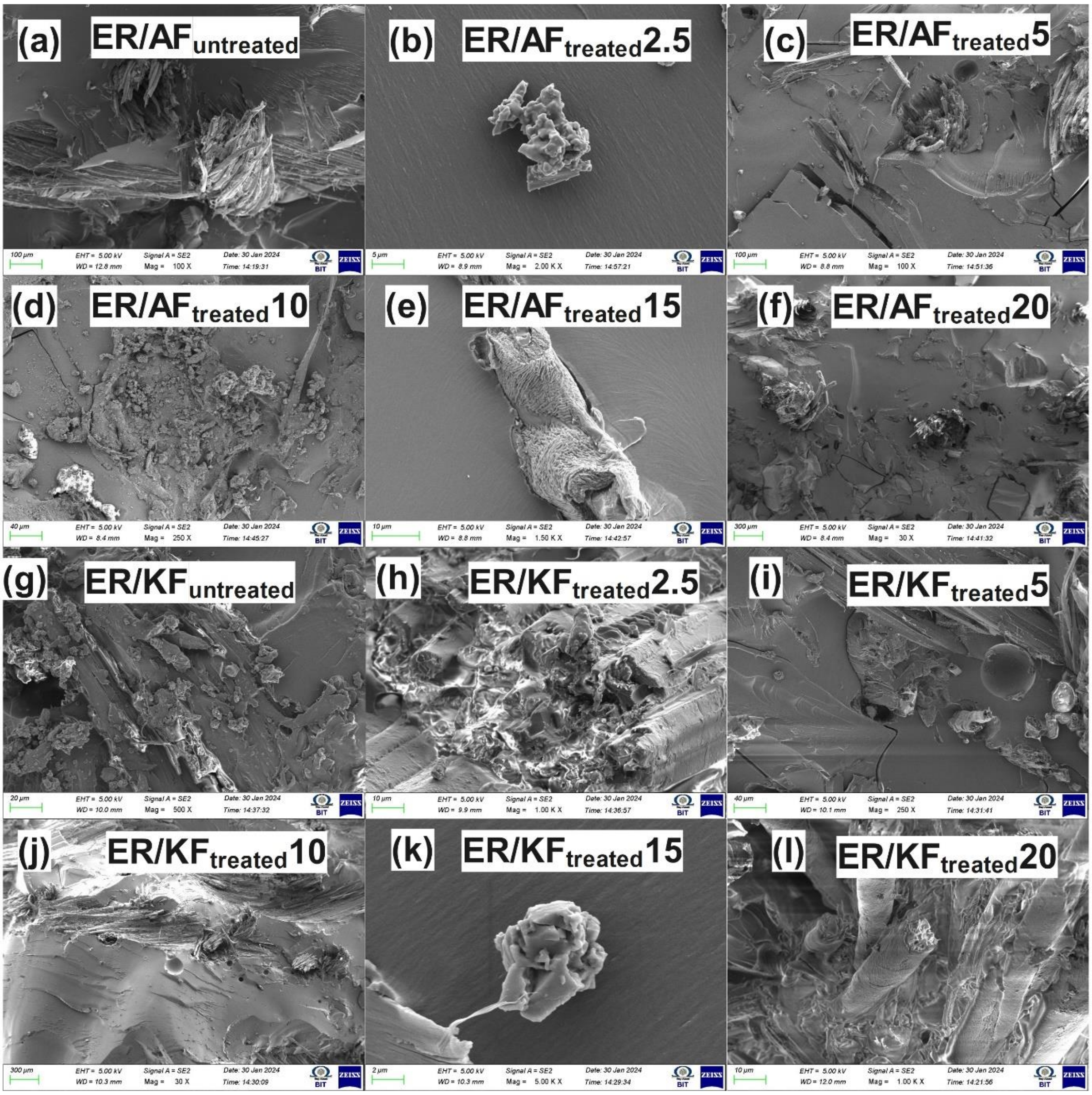

Figure 3. Scanning electron microscopic images of abaca and kenaf fiber treated and untreated - reinforced epoxy composites.

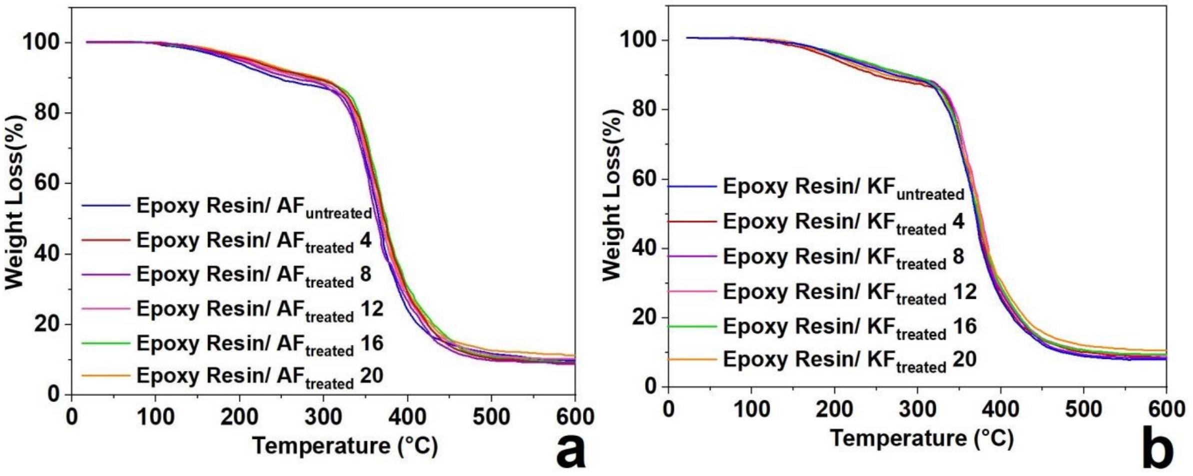

Figure 4. TGA graph of (a) AF-and (b) KF-reinforced epoxy composites.

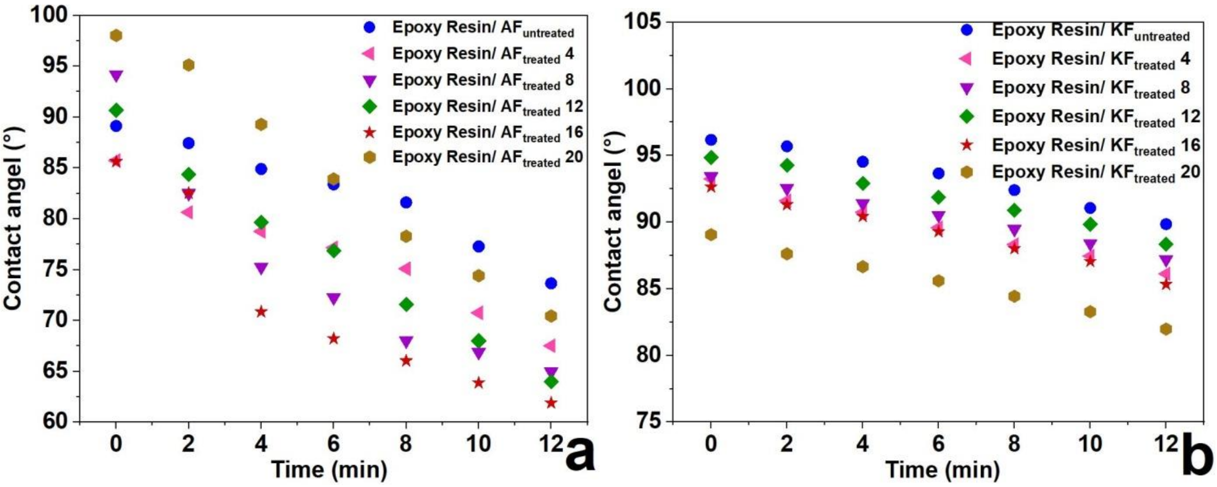

Figure 5. Contact angles between water droplets and fiber-reinforced composites with and without plasma treatment at 12 minutes: (a) AF and (b) KF.

Water Angle

As illustrated in Figure 5(a) and Figure 5(b), the composites' characteristics were determined by measuring the contact angle.

Automatic recording was carried out from 0 to 12 minutes after water droplets were deposited onto the composite surfaces. A contact angle of 72^{0} after 10 minutes was observed in the EP/AF$_{\text{untreated}}$ composite, which means that the surface wettability is low (Figure 5a). Because of the high polarity of the plasma treatment, the water contact angles of the treated samples decreased after 12 minutes as the treatment time increased (70.44, 64, 64.98, and 61.89°).

The water contact angles raised to 67^{0} after 20 minutes of treatment owing to the maximal degree of cross-linking and the effect of surface roughness from AF tr. Once the plasma treatment time was increased, the Epoxy/KF$_{\text{untreated}}$ composite's contact angle decreased from 85^{0} after 10 minutes (Figure 5b). The reduction of the WCA of the Epoxy/KF$_{\text{treated}}$ material indicates that the KF$_{\text{treated}}$ structure is hydrophilic, which is caused by the significant amount of −COOH and −OH groups generated. In contrast, because to the high cross linking density inside the epoxy matrix, the contact angle was greater for BR/AF tr that had been treated for 20 minutes compared to untreated AF tr. The FTIR analysis confirmed the cross linking reaction, and the TGA results verified that the amount of cross linking increased with treatment time. As the length of the DBD plasma treatment grew, the contact angles between the two composite fibers decreased. Reason being, after being exposed to Ar + O_2 gas, which etched the surface fibers, the amount of hydrophilic groups on the fibers, surface roughness, and porosity all increased. A decrease in the composite's water resistance and an increase in water accessing the fibers were both affected by the prolonged plasma treatment.

CONCLUSIONS

Plasma treatment with DBD Ar + O_2 allowed for the successful development of Epoxy/AF and Epoxy/KF. Epoxy composites bonded with abaca and kenaf fibers had their qualities greatly improved after being treated with Ar + O_2 gas plasma. In terms of tensile strength, Epoxy/AF treatment was superior, but Epoxy/KF treatment yielded far better elongational break. The FTIR analysis results validated the response among the epoxy groups and the C-O and -NH_2 groups of the plasma treatment, proving that the treated fibers exhibited better interaction bonding with the epoxy. Composites treated with Epoxy/AF and Epoxy/KF have improved flexural moduli and strengths owing to the improved surface roughness and polarity of the fibers caused by Ar + O_2 plasma treatment. Through the use of microscopy, the surface roughness and relatively less void among the fibers and the epoxy were brought to light. While the KFs exhibited outstanding interfacial adhesion and a small gap throughout treatment, the AFs showed a minor increase in surface roughness. The TGA further confirmed that the long-term Ar + O_2 plasma treatment enhanced thermal stability and reactivity, resulting in a notable reduction in weight. Because the plasma treatment made the fiber's surface more hydrophilic, etched, porous, and rough, and because the amount of hydrophilic groups increased, the WCA was lowered. There are a variety of packing, coating, building, and electrical uses for epoxy/$AF_{treated}$ and epoxy/$KF_{treated}$ composites.

REFERENCES

1. Habr, J., Lenfeld, P., Behalek, L., Boruvka, M. and Brdlik, P. (2020) Mechanical properties of biopolymer composite with natural fibers surface modified by low-temperature plasma.*MM Science Journal*, **2020**, 4007–4014.

2. Tanasă, F., Teacă, C.A., Nechifor, M. and Stanciu, M.C. (2022) Physical methods for the modification of the natural fibers surfaces. *Surface Treatment Methods of Natural Fibres and their Effects on Biocomposites*, 125–146.

3. Thangavel, P., Vignesh, S., Sureshkumar, R., Gowrishankar, A. and Girimurugan, R. (2023) Study on mechanical properties of polylactic acid matrix added with fly ash and tamarind kernel powder micro fillers. *NanoWorld J.*, **9**, S626–S630.

4. Shihab, M., Ibrahim, S.A., Mahmoud, S.A. and Noser, A.A. (2024) The impact of atmospheric air plasma treatment on the polyfunctional end-use polyester fabric using new synthetic pyrazole dye. *Dyes and Pigments*, **229**, 112302.

5. Jagatheesan, K. and Satheeshkumar, T. (2024) Mechanical properties of abaca fibre reinforced with recycled polypropylene composite. *Indian Journal of Fibre & Textile Research*, **49**, 237–245.

6. Manickam, T., Iyyadurai, J., Jaganathan, M., Babuchellam, A., Mayakrishnan, M. and Arockiasamy, F.S. (2023) Effect of stacking sequence on mechanical, water absorption, and biodegradable properties of novel hybrid composites for structural applications. *International Polymer Processing,* **38,** 88–96.

7. Kurien, R.A., Selvaraj, D.P., Sekar, M., Koshy, C.P., Paul, C., Palanisamy, S., Santulli, C. and Kumar, P. (2023) A comprehensive review on the mechanical, physical, and thermal properties of abaca fibre for their introduction into structural polymer composites. *Cellulose*, **30**, 8643–8664.

8. Balajikrishnabharathi, A. and Jayabalakrishnan, D. (2024) Characterization of mechanical, dielectric, EMI shielding properties of abaca bract biocarbon and pineapple fiber reinforced rigid vinyl ester composite. *Polymer Bulletin*, **81**, 12267–12285.

9. Alshahrani, H. and Vincent Rethnam, A.P. (2024) Effect of abaca bracts biocarbon volume and infill ratio on mechanical, wear, fatigue and hydrophobic behaviour of acrylonitrile butadienestyrene biocomposites tailored using 3D printing. *Fibers and Polymers*, **25**, 1087–1097.

10. Girimurugan, R., Rajasekaran, P., Loganathan, G. B., Gandhi, A. G., Anandaram, H. and Josep, R. E. (2024) Influence of E-Glass Fiber Addition on Mechanical Properties of Jute Fiber Reinforced Hybrid Composites. *International Journal of Vehicle Structures & Systems*, **16**, 723–727.

11. Ramanjaneyulu, C., Saravanan, S., Babu, G.D. and Prabhu, P. (2024) Study on the engineering properties of abaca/hemp/kenaf natural fiber mats reinforced with Anogeissus latifolia, polyester resin, and fly ash nano powder nanocomposites. *Biomass Conversion and Biorefinery*, 1–11.

12. Dani, M.S., Saravanan, N., Girisha, L., Uday, K.K., Ramalingam, R., Nanthakumar, S., Girimurugan, R., Anbarasu, M. and Mathanbabu, M. (2024) Optimizing the Properties of AA 5052 Alloys through Silicon Carbide and Groundnut Shell Ash Reinforcements. International Journal of Vehicle Structures & Systems, **16,** 630–635.

13. Venkatasudhahar, M., Velu, R., Dilip Raja, N. and Logesh, K. (2020) Experimental investigation on

natural fibre composite for thermal insulation performance enhancement. *International Journal of Ambient Energy*, **41**, 1304–1307.

14. Appusamy, A. M., Laxmanan, S. K., Subramaniyan, M., Maheskumar, P., Kumar, K. S. and Girimurugan, R. (2024) A Critical Review on Polymer Composites Reinforced with Artificial Fibers using Fused Deposition Modelling. *J. Environ. Nanotechnol.*, **13**, 440–448.

15. Jeyaprakasam, S., Gnanasekaran, M., Magibalan, S., Singh, R.P., Mohanavel, V., Kannan, S., Giri, J., Ali, M.S. and Barmavatu, P. (2024) Tribological, mechanical and microstructure characteristics of hybrid aluminium matrix composite containing titanium carbide (TiC) and graphite particles. Journal of Materials Research and Technology, **33,** 5482–5489.

16. Ponnuswamy, M., Sathishkumar, T.P., Selvaraju, M. and Sundramurthy, V.P. (2024) Ensetventricosum Fibre-Based Biocomposite Preparation with Wood Apple Shell Particles as a Filler: Effect of Alkali Treatment and Optimization of Composition for Physio-Mechanical Properties. *Arabian Journal for Science and Engineering*, **49**, 15733–15748.

17. Sinha, A.K., Bhattacharya, S. and Narang, H.K. (2021) Abaca fibre reinforced polymer composites: a review. *Journal of Materials Science*, **56**, 4569–4587.

18. Shakir, M.H. and Singh, A.K. (2024) Repercussion of fiber content on the mechanical, thermal, and thermomechanical properties of natural fibers reinforced thermoplastic composites for automotive application. *Physica Scripta*, **99**, 095914.

19. Moorthy, A., Kanagaraj, K., Palanisamy, M. and Ramasamy, G. (2024) Investigation of synthetic and natural cork fiber laminate polymer composite bending characteristics. *Matéria (Rio de Janeiro),* **29**, e20240489.

20. Rosli, N.A., Khairudin, F. A., Kargarzadeh, H., Othaman, R. and Ahmad, I. (2022) Hydrophobic-oleophilic gamma-irradiated modified cellulose nanocrystal/gelatin aerogel for oil absorption. *International Journal of Biological Macromolecules*, **219**, 213–223.

21. Marwan, M., Indarti, E., Bairwan, R.D., Khalil, H.A., Abdullah, C.K. and Ahmad, A. (2024) Enhancement micro filler spent coffee grounds in catalyst-chemically modified bast fibers reinforced biodegradable materials. *Bioresource Technology Reports*, **25**, 101723.

22. Ramanjaneyulu, C., Somasundaram, S., Babu, G.D. and Shajahan, M.I. (2024) Experimental investigation of mechanical, thermal, DMA analysis and morphological analysis on Abaca/Hemp/Kenaf reinforced with Anogeissus latifolia blender polyester nanocomposites. *Matéria (Rio de Janeiro)*, **29**, 20240380.

23. Mayakannan, S., Raj, J.B. Raja, V.L. and Nagaraj, M. (2023) Effectiveness of silicon nanoparticles on the mechanical, wear, and physical characteristics of PALF/sisal fiber–based polymer hybrid nanocomposites. *Biomass Conversion and Biorefinery*, **13**, 13291–13305.

24. Nadhari, W.N.A.W., Danish, M., Abdullah, S.N.A.B., Alanazi, A.M., Abd Karim, N. and Mustapha, A. (2024) Effect of potato starch on surface characteristics, mechanical, physical, and chemical binding mechanism of kenaf binderless particleboard. *Industrial Crops and Products*, **212**, 118300.

25. Venkatasudhahar, M., Ravichandran, A.T. and Dilipraja, N. (2022) Effect of stacking sequence on mechanical and moisture absorption properties of abaca-kenaf-carbon fiber reinforced hybrid composites. *Journal of Natural Fibers*, **19**, 7229–7240.

26. Senniangiri, N., Gokulkannan, I.S., Kumar, I.S.D. and Gokul, I.S. (2025) Enhancing Mechanical, Moisture Resistance, and Fire-retardant Properties of Nelumbo nucifera Fiber/Epoxy Nanocomposites with Zinc Oxide Nanoparticles. *J. Environ. Nanotechnol.*, **14**, 253–265.

27. Priya, V.N., Rajkumar, M., Rajendran, V., Mobika, J., Sibi, S.L., Veena, B., Vijayalakshmi, V. and Ahila, P. (2025) Sustainable selenium ions adsorption of cyclodextrin and cellulose functionalized layered double hydroxide/reduced graphene oxide nanocomposites. *Journal of Water Process Engineering,* **69**, 106580.

28. Kumar, K.S., Sundaram, K., Anand, S., Vijayalakshmi, M., Logesh, M., Anbarasu, D., Asha, I. and Kannapiran, N. (2024) Synthesis, magnetic and dielectric properties of poly (m-phenylenediamine)/$ZnNiFe_2O_4$ nanocomposites. *Inorganic Chemistry Communications*, **161**, 111983.